

Further Testing/Validation of the Satellite f/Q correction in Case 1 waters

Kenneth J. Voss, Nordine Souaidia, and Albert Chapin
Department of Physics, Univ. of Miami, Coral Gables, Fl. 33124

Andre Morel and David Antoine
Laboratoire d'Océanographie de Villefranche,
Université Pierre et Marie Curie et Centre National de la Recherche Scientifique,
BP 8, F 06238 Villefranche-sur-mer, France

INTRODUCTION

The upwelling radiance distribution is not isotropic, but varies with illumination and viewing conditions and water optical properties. Knowledge of this angular variation is important in satellite oceanography, as the analysis of satellite derived upwelling radiances must take into account these variations. This is particularly important when comparing different satellite systems (matchup data bases) as different satellites will view the same spot at different times (hence varied illumination geometry) and different view angles. One must have a model of this variation of the radiance distribution that is dependent on a small set of parameters, but which can accurately predict the variation.

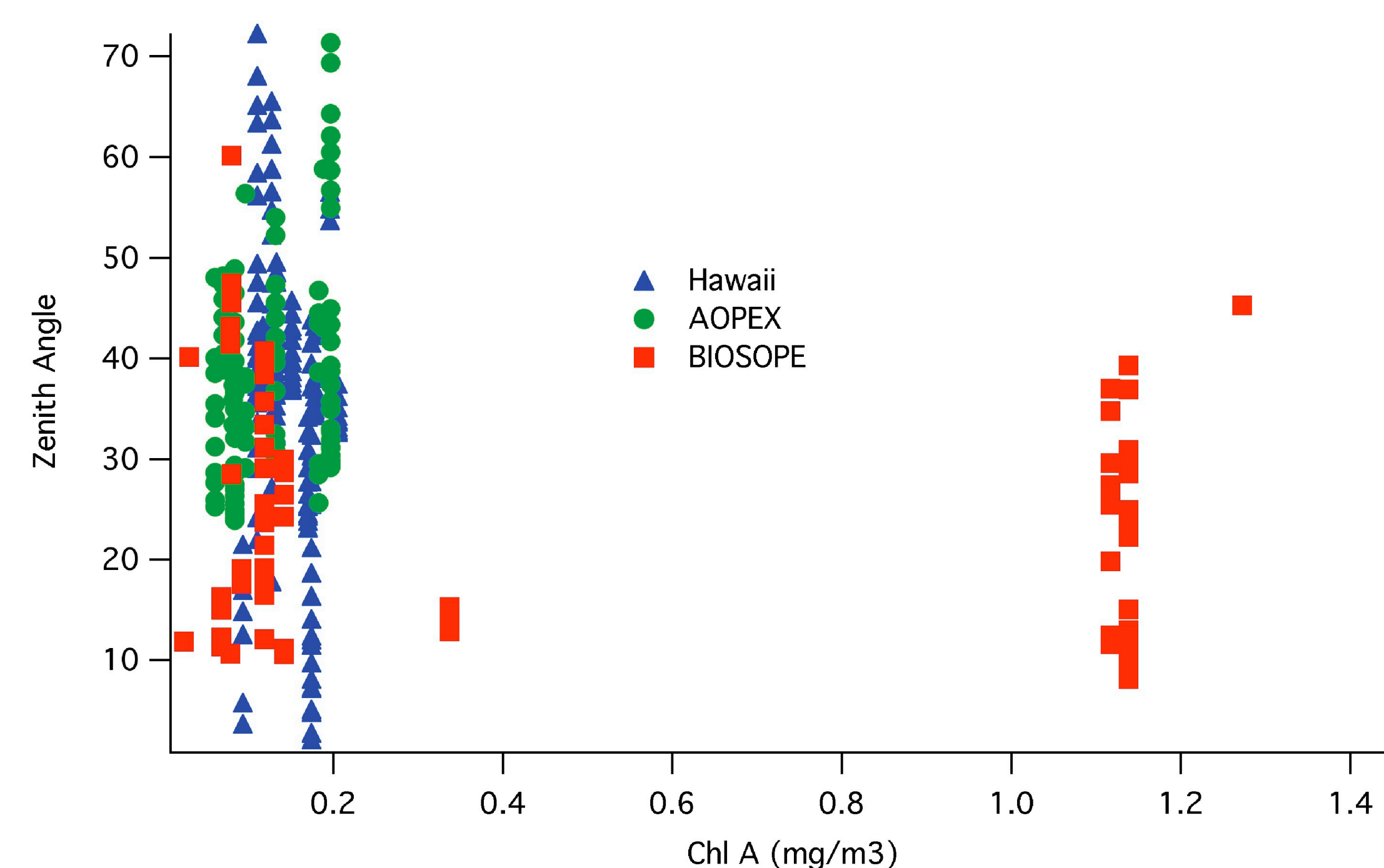
The shape of the upwelling radiance distribution can be defined in terms of the $Q(\theta_o, \theta_v, \phi_v)$ which is defined as $Q(\theta_o, \theta_v, \phi_v) = E_u(\theta_o) / L_u(\theta_o, \theta_v, \phi)$ where θ_o is the solar zenith angle, θ_v is the view zenith angle and ϕ is the azimuth between these two directions. The current model which is used in satellite oceanography to characterize this variation in Q is the model by Morel et al. (2002). This model incorporates both a correction for this Q factor, and also a correction for the f factor, which relates the irradiance reflectance to the inherent optical properties of bb and a ($f = bb / (a + bb)$). This paper will very briefly describe our results in validating the Q factor alone, as we do not have a large data base of bb or a .

In the past we have had two investigations looking at the accuracy of the series of Morel f/Q models (Morel et al. 1995; Voss and Morel, 2005). Each of these was done with a different version of our radiance distribution camera systems (RADS: Voss, 1989; RADS-II, Voss and Chapin, 1992). These early instruments were large and slow, thus provided a limited data set. Recently we have developed a new generation of radiance distribution camera systems specifically aimed at looking at the upwelling radiance distribution (NuRADS: Voss and Chapin, 2005). With this instrument we have an extensive set of upwelling radiance distribution data in both Case I and Case II waters. This paper will concentrate on the Case I waters, where the Morel model is supposed to work.

DATA DESCRIPTION

We will concentrate on 2 specific cruises, in the South Pacific and Mediterranean, and several short cruises near Hawaii. The BIOSOPE cruise in the South Pacific had a variety of water types from very, very clear ($chl < 0.05$ mg/m³) to coastal ($chl > 1$ mg/m³). The AOPEX cruise took place in the Mediterranean, and while the water types were not as varied, we had the opportunity to sample the radiance distribution for a variety of solar zenith angles. In addition to these two cruises, we have an extensive set of radiance distribution measurements in clear waters around Hawaii (chl approximately 0.1 mg/m³). All of these measurements were done just below the surface (at approximately 0.75 m).

This figure illustrates the range of Chl A and Zenith angle for the radiance distribution data presented in this paper. This is for one wavelength (490 nm), similar data exists for most of the other wavelengths. The Hawaii data set has points in the range < 0.2 mg/m³ Chl A, but has a large range of zenith angles, from almost 0 to over 70 degrees. The AOPEX data is over a similar Chl A range (< 0.2 mg/m³) but a slightly more limited zenith angle range ($20 < \text{Zenith angle} < 75$ degrees). The BIOSOPE data from the South Pacific has a wider range of Chl A, from < 0.05 to > 1.4 mg/m³. But this data set does have a large hole in the range from 0.4 to 1.0 mg/m³.

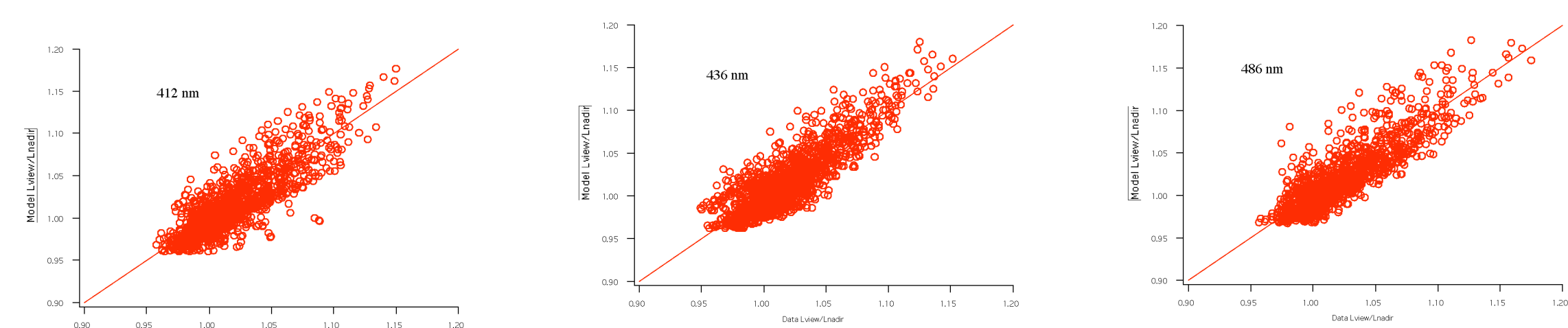


DATA REDUCTION

The NuRADS instrument obtains a complete spectral set of data every 2 minutes. However, since the whole upwelling radiance distribution is obtained very quickly (less than 1 sec), individual images often have strong features, such as wave focusing, which need to be averaged out. During the data reduction process we look at each image and determine, manually, where the anti-solar point is located. This point is obvious as it is the center of where the wave focusing light rays converge. Once this point has been determined, a routine determines where the nadir point should be, given the illumination geometry and the symmetry around the principal plane. When the geometry has been determined, we take an average of images taken within 10 minutes. For the data presented in this paper, we exclude data for which only one image (both halves) are averaged, so each data point effectively represents the average of between 4 and 10 separate images. Our comparison is between L_{view}/L_{nadir} for the data and that predicted by the Morel et al. (2002) model. We use Chl determined separately to enter into the Morel tables, but use illumination geometry as determined by the specific case.

RESULTS

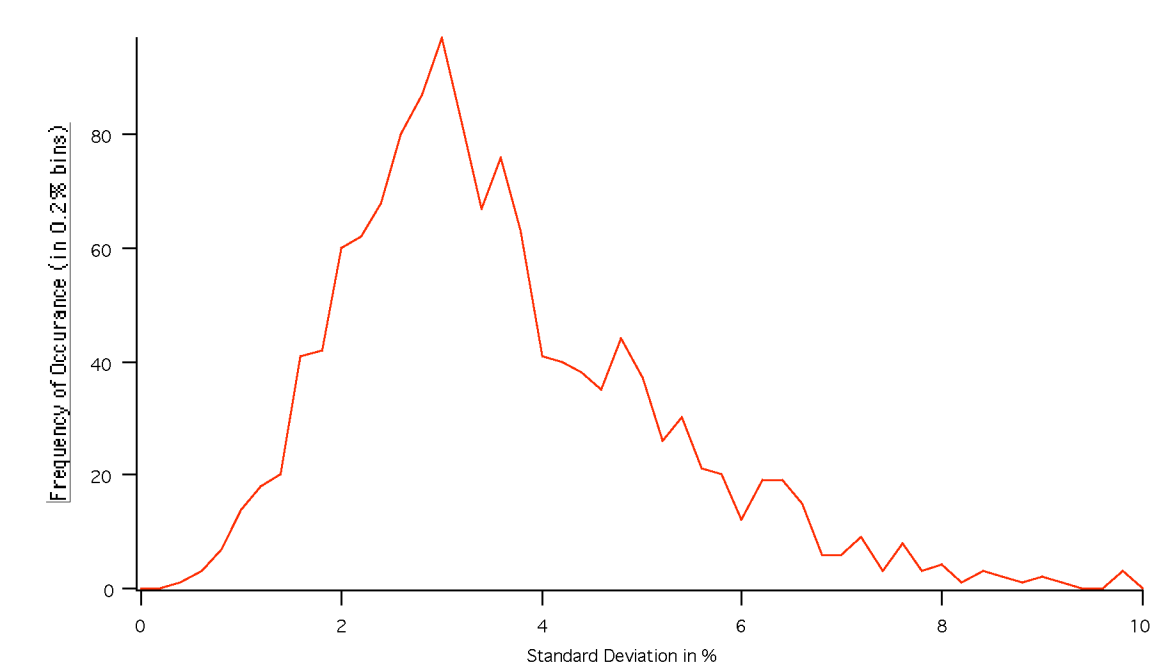
Typical results are shown as below for one day during the BIOSOPE cruise (12/1/04).



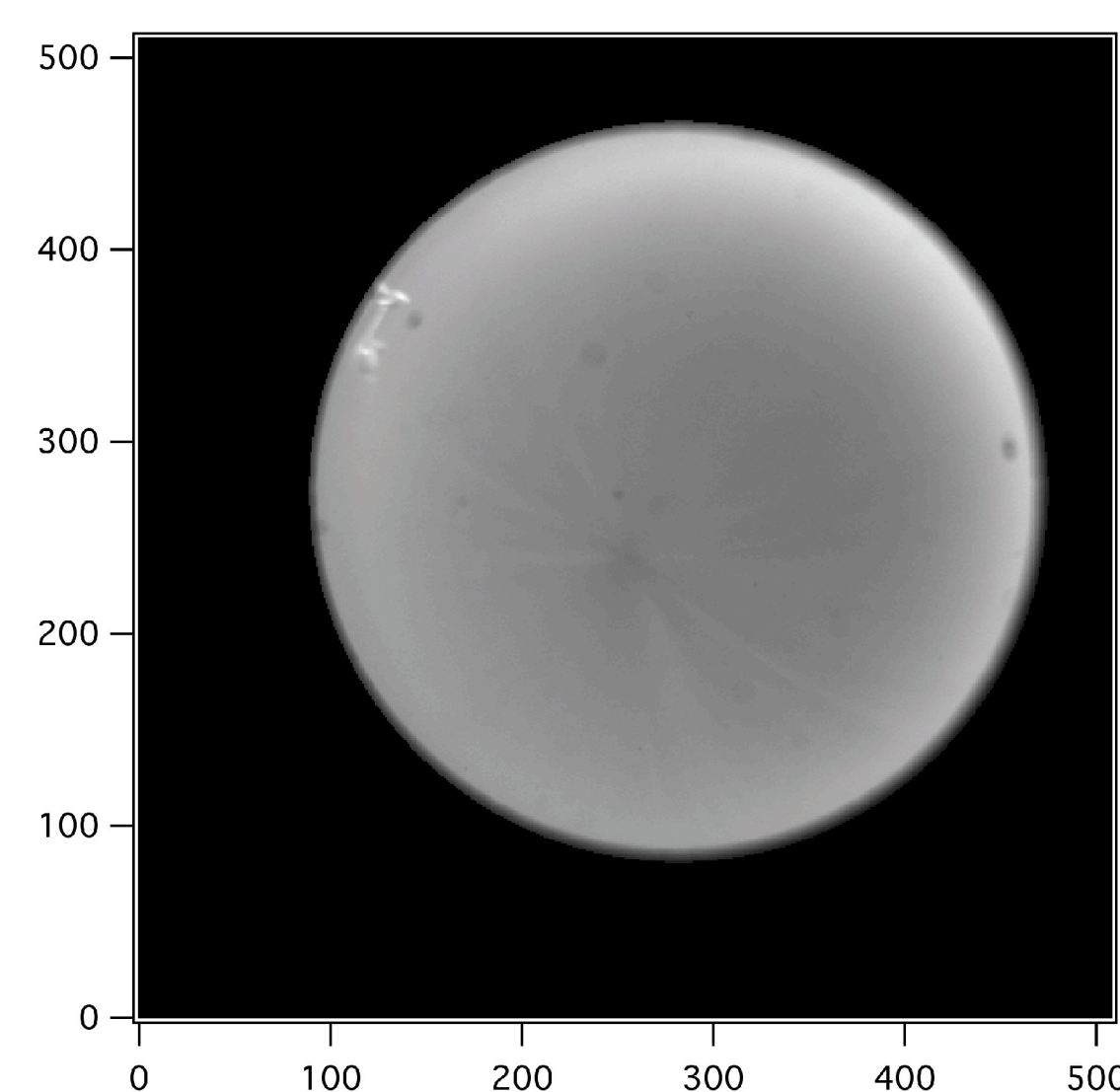
Each data point represents a different direction or data set in that day. The resolution of direction is every 5 degrees in nadir and 15 degrees in Azimuth, thus there can be approximately 8 (5-40 degrees in nadir) x 12 (0 - 180 degrees in azimuth) = 96 points from each radiance distribution data set. For each day we calculated the deviation between the model and data using :

$$\text{Error} = \text{sum}(\text{data-model})/N$$
$$\text{RMSE} = \text{Sqrt}(\text{sum}(\text{data-model})^2/N)$$

For this data set the error was < 0.01 , while the RMSE was < 0.02 . In general the RMSE from 0.01 to 0.04, but was mostly on the order of 0.02-0.03. The largest RMSE tends to be towards the longer wavelengths where increased shadowing may be causing problems in the data. However, another factor must be taken into account. Noise in the light field will show up in this comparison as an error between the model and the data. Below we show a histogram of the standard deviation of the average for each point in the above comparison. This variability is both from small errors in determining the image geometry, and natural variability due to wave focusing and other factors. This specific case is for 486 nm, for the data shown above in the model-data comparison.

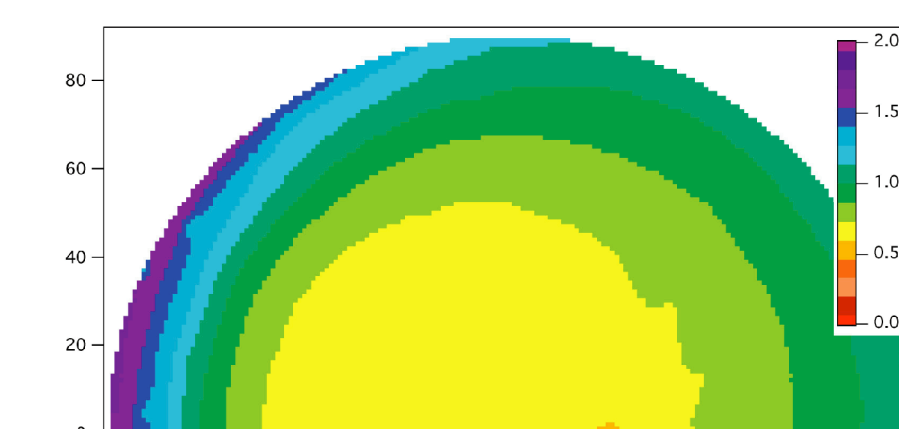


As can be seen the data has variations on the order of 3%. This then limits how well a model might represent the data, and explains some of the variability of the data around the model prediction (shown as the 1:1 lines in Fig. 2).

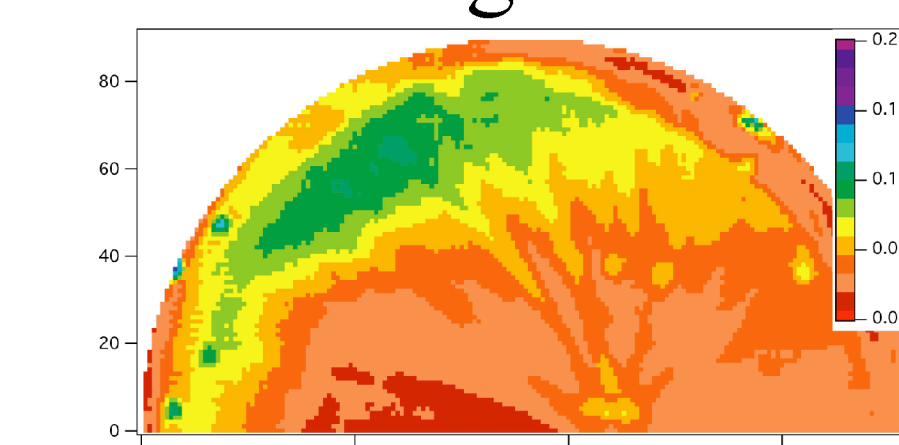


Example image, 520 nm.

Part of the explanation for the noise can be found from the transformation from the image on the left to the images on the right. The image on the left is an individual upwelling radiance distribution. Note wave focusing, among other features. In the averaging process the image on the left, along with all others at this wavelength and within 10 minutes are averaged to form the radiance distribution on the right. Note how the image appears smooth, with the wave focusing not here. However the image below the average is the % std of the individual pixels going into the average. Here one can see that the wavefocusing has caused a lot of variation in the average. As can be seen, the natural environmental noise can cause a variability that will affect how well the model agrees with the data.



Average



% Standard Deviation

CONCLUSION

The Morel et al. (2002) model does a very good job of reproducing the radiance distribution variations that we see in our data set for Case I waters and explains most of the variation in the shape of the radiance distribution. However each real, measured, radiance distribution has many features in it due to wave focusing, and downwelling illumination variations. As such, while the model does a good job at predicting the average, it will never exactly fit a measured radiance distribution (nor should it be expected to do this). Much more work needs to be done to move this Case I model into the Case II regime. We currently are looking at this Case II situation with 2 data sets collected in the Chesapeake Bay, and are also looking into issues of the polarization of the upwelling light field.

REFERENCES

- Morel, A., D. Antoine, and B. Gentili. 2002. Bidirectional reflectance of oceanic waters: Accounting for Raman emission and varying particle scattering phase function. *Appl. Opt.* 41: 6289-6306.
- Morel, A., K. J. Voss, and B. Gentili, 1995. Bi-directional reflectance of oceanic waters: A comparison of model and experimental results. *J. Geophys. Res.*, 100: 13,143-13,150.
- Voss, K. J. 1989. Electro-optic camera system for measurement of the underwater radiance distribution. *Optical Engineering*, 28: 241-247.
- Voss, K. J. and A. L. Chapin. 1992. Next generation in-water radiance distribution camera system. *Proc. Soc. Photo-Optical Instrumentation Engineers*, 1750: 384-387.
- Voss, K. J. and A. L. Chapin. 2005. Upwelling radiance distribution camera system, NURADS. *Optics Express*, 13: 4250 - 4262.
- Voss, K. J. and A. Morel. 2005. Bidirectional reflectance function for oceanic waters with varying chlorophyll concentrations: Measurements versus predictions. *Limnology and Oceanography* 50: 698-705.